Applications of Contact Length Models in Grinding Processes

H.S. Qi[1,a], B. Mills[2] and X.P. Xu[3,b]

[1]University of Bradford, UK

[2]Liverpool John Moores University, UK

[3]Huaqiao University, China

[a]h.qi@bradford.ac.uk; [b]xpXu@hqu.edu.cn

Keywords: Grinding, Contact length, Criterion for Model Simplification

Abstract. The nature of the contact behaviour between a grinding wheel and a workpiece in the grinding process has a great effect on the grinding temperature and the occurrence of thermal induced damage on the ground workpiece. It is found that the measured contact length l_e in grinding is considerably longer than the geometric contact length l_g and the contact length due to wheel-workpiece deflection l_f. The orthogonal relationship among the contact lengths, i.e. $l_c^2 = (R_r l_f)^2 + l_g^2$, reveals how the grinding force and grinding depth of cut affect the overall contact length between a grinding wheel and a workpiece in grinding processes. To make the orthogonal contact length model easy to use, attempts on modification of the model are carried out in the present study, in which the input variable of the model, F_n', is replaced by a well-established empirical formula and specific grinding power. By applying the modified model in this paper, an analysis on the contributions of the individual factors, i.e. the wheel/worpiece deformation and the grinding depth of cut, on the overall grinding contact length is conducted under a wide range of grinding applications, i.e. from precise/shallow grinding to deep/creep-feed grinding. Finally, using a case study, the criterion of using geometric contact length l_g to represent the real contact length l_c, in terms of convenience versus accuracy, is discussed.

Introduction

The contact length between a grinding wheel and a workpiece during grinding processes is one of the principal factors that contribute to the quality of the ground workpiece from either thermal or mechanical aspects, since it determines the bottom length of the heat source and interface force distributions and consequently it affects the intensity of the energy flux into the workpiece, the peak temperature and the rate of wear of the grinding wheel [1, 2, 3, 4]. Although the geometrical contact length l_g has been widely used as a measure of the real contact length l_e, it is well known that the measured/real contact lengths could be up to many times that of the geometrically calculated lengths [4-11]. Much effort has been made to understand the mechanism of the contact deformation between a wheel and a workpiece and to quantify the real contact length through analytical/numerical modelling and experimentation.

In the present work, a review on the research carried out in the past decades on contact length modelling is carried out. The orthogonal contact length model developed by Rowe and Qi [11] is then modified in order to make it easier to use in practice. In the second part of this paper, some application cases of the orthogonal contact length models are presented. By using the modified orthogonal contact length model, the difference between the overall contact length and the geometrical contact length as well as the difference between the overall contact length and the contact length due to grinding force are analysed under a wide range of grinding conditions. Furthermore, with a case study, the criterion of using geometric contact length l_g to represent the real contact length l_c, in terms of convenience versus accuracy, is discussed. Finally, the effect of wheel wear on the grinding temperature is discussed with the help of the modified orthogonal contact length model.

Review of the Contact Length Models

The mechanisms of the contact deformation between a wheel and a workpiece and quantification of the real wheel/workpiece contact length have been investigated through analytical/numerical modelling and experimentation in the past decades. A comprehensive review on the researches and the model developments in grinding contact lengths was given by Zhang [4]. Table 1 includes some of the published contact length models [4-11]. Depending on the assumptions used in the modelling, the contact length models can be categorised into three types. In the first type of models, represented by the works of Lindsay/Hahn [5], and Brown/Saito/Shaw [6], Hertz contact theory was used in calculating the contact length due to grinding forces. The geometrical effect of the wheel depth of cut on the contact length, however, was assumed to be negligible. The models of this type revealed the importance of grinding wheel hardness or its elastic modulus on grinding contact length. In contrast, the second type of models considered the geometry effect, i.e. the effects of the wheel depth of cut and the wheel diameter, on the contact length, but neglected the effect of the grinding force and the wheel-workpiece deformation. The advantage of the contact length models of this type is that it is simple and easy to use, which is the main reason for using the geometrical contact length l_g to represent the overall contact length l_e. In the third type of the models, such as those introduced by Kumar/Shaw [7], Hideo [8], and Zhang [4], the local wheel-workpiece deformation and the wheel depth of cut were considered as two equally important factors on the overall grinding contact length. The third type of models revealed the reason why l_e was much larger than l_g. In addition, the possible effects of the surface roughness of the workpiece and the topography of the grinding wheel on the overall contact length were studied by Brandin [9], who proposed that the difference between geometric contact length and the real contact length was due to the geometrical effect of the surface roughness of the workpiece. In contact mechanics, as explained by Greenwood [12], the topography of the surfaces in contact is of primary importance. The contact length between two rough surfaces in contact is greater than the contact length between two smooth surfaces in contact under the same contact force. Peklenik [13] characterised the stochastic nature of the grinding process arising from the randomness of the distribution of cutting edges in the grinding wheel surface when measuring grinding temperature. To clarify the complex relationship one needs to understand the principle of the deformation of a wheel-workpiece system at macroscopic as well as microscopic levels.

The contact length model developed by Rowe/Qi [11, 14 - 15] clarified the orthogonal effects of the wheel-workpiece deformation, the grinding geometry and the topography of the rough wheel-workpiece contact surfaces on the overall contact length of the grinding contact zone. The orthogonal contact length model is represented in Eq.(1):

$$l_c^2 = l_{rf}^2 + l_g^2 = (R_r l_f)^2 + l_g^2 \tag{1}$$

where

$$l_g = (a_e\, d_e)^{0.5} \tag{1a}$$

$$l_f = [8\, F_n' (K_s + K_w)\, d_e]^{0.5} \tag{1b}$$

$$1/d_e = 1/d_s \pm 1/d_w,$$

$$K_s = \frac{(1 - \upsilon_s^2)}{\pi E_s},\quad K_w = \frac{(1 - \upsilon_w^2)}{\pi E_w}$$

Formula (1a) defines the geometric contact length, l_g, based on the grinding geometry theory, and Formula (1b) defines the contact length due to grinding force, l_f, based on Hertzian contact theory. In addition, considering the fact that the contacting surfaces in abrasive machining processes are far from ideal smooth contact, a roughness factor R_r is introduced in Eq.(1). The detail of the derivation of the contact length model can be found in the reference [16].

In Eq.(1), the roughness factor R_r, is a constant, i.e. it's not sensitive to the process parameters. A detail study on R_r was carried out, which can be found in [16]. $R_r = 9$ is used in the present study. E_s and E_w are the moduli of elasticity of the grinding wheel and of the workpiece respectively. υ_s and υ_w are the Poisson ratios of the grinding wheel and the workpiece respectively. These properties are available from standard material handbooks. The grinding process parameters, which include d_e, the equivalent diameter of the grinding wheel, d_s, the diameter of the grinding wheel, d_w, the diameter of the workpiece, and a_e, the real depth of cut, are available for particular grinding application.

The specific normal force F_n' in Eq.(1), however, is normally not always available or easy to obtain in actual grinding systems because that normally a special force measurement system is required for obtaining the value of F_n'. In next section, the Formula (1b) in the Eq.(1) is modified by using specific grinding power, which is much easy to obtain, and by a well established grinding force model to replace the input variable F_n'.

Table 1 A summary of typical grinding contact length models published

Model	l_c/l_g	Contact length l_c	Comment
Lindsay[5]	1.33	$10^{-6}\sqrt[3]{\frac{d_e^2 F_n'}{d_g^2(1.33HL+2.2SL-8)}}$	Disregards depth of cut
Brown[6]	2.0-2.9	$2\sqrt{A\,d_s}\,\sqrt[3]{\frac{F_n'}{d_g^2 l_c M}}+B\sqrt{F_n}$	Disregards depth of cut
Kumar[7]	1.1-1.2	$\alpha\beta l_g = \alpha\beta\sqrt{a\,d_s}$	Smooth body elastic contact
Hideo[8]	1.2-1.3	$\sqrt{(a+\delta_t)\,d_e}+\sqrt{\delta_t\,d_e}$	Smooth body elastic contact
Brandin[9]	1.1-2.9	$\sqrt{(a+R_t)\,d_s}+\sqrt{R_t\,d_s}$	Roughness effect on depth of cut
Maris[10]	2	$\sqrt{a\,d_s}\,q^{-0.216}e^{[-0.0205q^{0.33}\ln a]}$	Empirical
Zhang [4]		$R_d = \arccos(1-a_c/R_d)$	
Rowe/Qi [11]		$l_c^2 = (R_r l_f)^2 + lg^2$	

Modifications of the Orthogonal Contact Length Model

Use of Grinding Power. In a practical grinding system, the grinding power signal is much easier to obtain in the course of a grinding operation, in comparison with the grinding force signal. For a plunge grinding operation the specific grinding power can be approximately related to the normal grinding force as:

$$P' \approx v_s F_t' = v_s \mu F_n', \tag{2}$$

where P' is specific grinding power, F_t' is specific tangential force and μ is the grinding friction coefficient, which is approximately 0.3 to 0.5. The specific normal force then is:

$$F_n' = F_t'/\mu = P'/(v_s \mu) \tag{3}$$

By using Eq.(3), Formula (1b) becomes Formula (1b'):

$$l_f = [8 P'(K_s + K_w)d_e/(v_s\mu)]^{0.5} \tag{1b'}$$

This modified contact length model is easy to use especially for on-line grinding process controls.

Use of an Empirical Force Model. Eq.(4) is Werner's empirical model for grinding force, which is used in this study [17]:

$$F_n' = F_0\, q^{(-e1)}\, a_e^{e2}\, d_e^{(e3)} 10^{(3\, e2)} \qquad (4)$$

where F_0, e_1, e_2 and e_3 are constants. F_0 is usually found to lie in the range 10 to 20 N/mm. e_1 is within 0 to 1 and the typical value is 0.55. e_2 is in the range 0.5 to 1 approximately and the typical value is 0.75. e_3 is in the range 0 to 0.5 and the typical value is 0.25 [17]. Furthermore, e_1, e_2 and e_3 are related by

$$e_1 = 2e_2 - 1 \text{ and } e_3 = 1 - e_2 \qquad (5)$$

Equations (4) and (5) have been verified for a wide range of grinding conditions, from fine grinding to creep feed grinding, from easily ground material to difficult to grind material [17]. By using the grinding force model Equations (4) and (5), Formula (1b) becomes Formula (1b''):

$$l_f = [8\, F_0\, q^{(-e1)}\, a_e^{e2}\, d_e^{(1+e3)} 10^{(3\, e2)} (K_s + K_w)]^{0.5}$$
$$= [8\, F_0\, q^{(1-2\, e2)}\, a_e^{e2}\, d_e^{(2-e2)} 10^{(3\, e2)} (K_s + K_w)]^{0.5} \qquad (1b'')$$

The orthogonal contact length model modified with the empirical force equation is, therefore, represented by the following equation:

$$l_c^2 = l_{rf}^2 + l_g^2 = (R_r\, l_f)^2 + l_g^2$$
$$= R_r^2\, 8\, F_0\, q^{(-e1)}\, a_e^{e2}\, d_e^{(1+e3)} 10^{(3\, e2)} (K_s + K_w) + a_e\, d_e$$
$$= R_r^2\, 8\, F_0\, q^{(1-2\, e2)}\, a_e^{e2}\, d_e^{(2-e2)}\, 10^{(3\, e2)}\, (K_s + K_w) + a_e\, d_e \qquad (6)$$

Applications of the Modified Orthogonal Contact Length Models

Study of the Difference between l_c and l_g. Eq.(7) is the contact length ratio between the real contact length and the geometrical contact length, $r_{c\text{-}g}$ derived based on Eq.(6) and Formula (1a):

$$r_{c\text{-}g} = l_c/l_g$$
$$= [1 + R_r^2\, 8\, F_0\, q^{(1-2\, e2)}\, a_e^{(e2-1)}\, d_e^{(1-e2)}\, 10^{(3\, e2)}\, (K_s + K_w)]^{0.5} \qquad (7)$$

Applying Eq.(7) with $R_r = 9$, $e_2 = 0.75$, $F_0 = 15$ N/mm, $(K_s+K_w) = 7.52\ 10^{-6}$ mm^2/N, the variation of the contact length ratio $r_{c\text{-}g}$ under a range of grinding conditions is obtained as shown in Figures 1 and 2. The base plane in the figures represents the real contact length equal to the geometrical contact length, i.e. $r_{c\text{-}g} = 1$. The curved face is $r_{c\text{-}g}$ as a function of speed ratio, q, and real depth of cut, a_e. Under a conventional grinding condition as shown in Figure 1, where q is from 50 to 300 and a_e is from 0.005 to 0.02 mm, the real contact length l_c is two times or more the geometrical contact length l_g. In addition, $r_{c\text{-}g}$ decreases as a_e and q increase, which indicates that the difference between l_c and l_g became smaller towards larger depth of cut and higher speed ratio, a scenario of creep feed grinding. As shown in Figure 2, under a creep feed grinding region, where q = 500-1000 and a_e = 1-15 mm, the magnitude of the geometrical contact length l_g is approaching that of the real contact length l_c.

Studay of the Difference between l_c and l_{rf}. Similarly, Eq.(8) is the contact length ratio between the real contact length and the contact length due to grinding force and the surface roughness factor, $r_{c\text{-}rf}$, derived based on Eq.(6) and Formula (1b''):

$$r_{c\text{-}rf} = l_c/l_{rf} = l_c/(R_r l_f)$$
$$= \{1 + [R_r^2\, 8\, F_0\, q^{(1-2\, e2)}\, a_e^{(e2-1)}\, d_e^{(1-e2)}\, 10^{(3\, e2)}\, (K_s + K_w)]^{-1}\}^{0.5} \qquad (8)$$

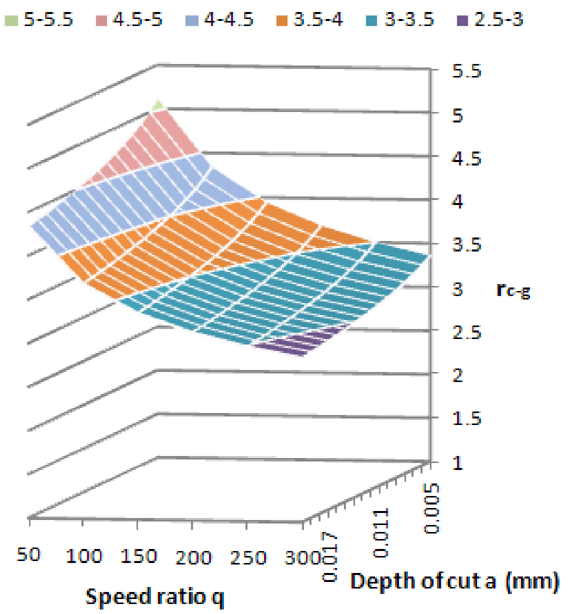

Fig.1 Ratio of real contact length over geometrical contact length under conventional grinding conditions, i.e. q = 50 -300; a = 0.005-0.02mm

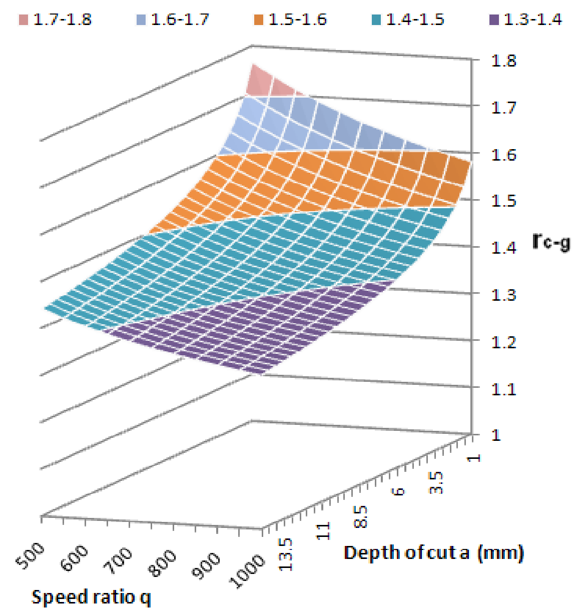

Fig. 2 Ratio of real contact length over geometrical contact length under creep feed grinding conditions, i.e. q = 500-1000; a=1-15mm

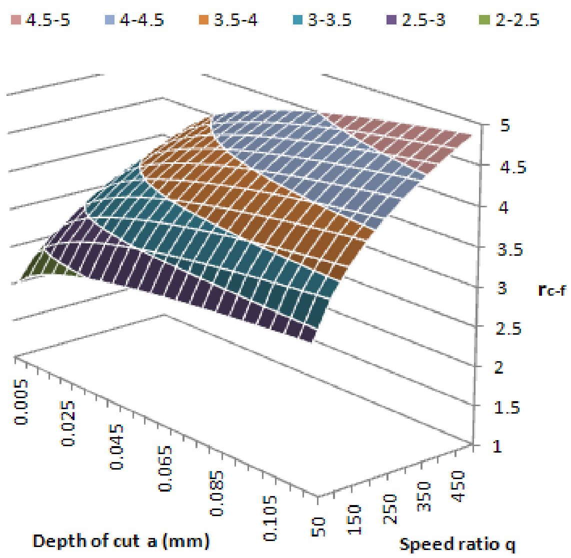

Fig. 3 Ratio of real contact length over the contact length due to grinding force only (i.e. R_r=1) under conditions of conventional grinding, i.e. q = 50 -500; a = 0.005- 0.12mm

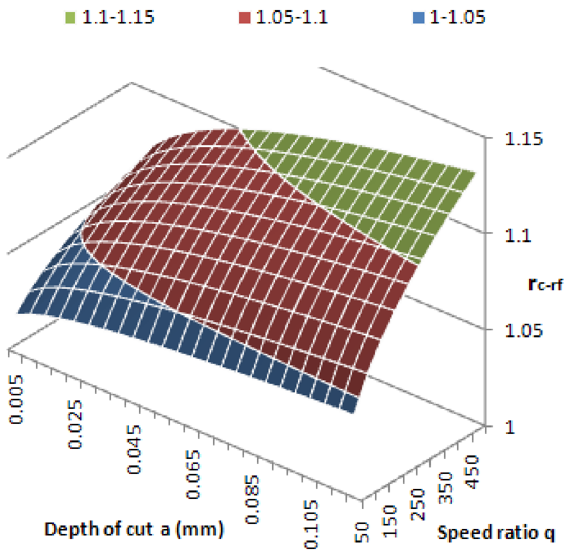

Fig. 4 Ratio of real contact length over the contact length due to grinding force and contact surface roughness (R_r=9) under conditions of conventional grinding, i.e. q = 50 -500; a = 0.005- 0.12mm

Applying Eq.(8) with e_2 = 0.75, F_0 = 15 N/mm, (K_s+K_w) = 7.52 10^{-6} mm^2/N, the variation of the contact length ratio $r_{c\text{-}rf}$ under a range of grinding conditions is obtained as shown in Figures 3 and 4. The base plane in the figures represents the real contact length equal to the contact length due to the force and roughness factor, i.e. $r_{c\text{-}rf}$ = 1. The curved face is $r_{c\text{-}rf}$ as a function of speed ratio, q, and real depth of cut, a_e. In Figure 3, the roughness factor R_r=1 is assumed, which means that the curved face represented the ratio of l_c and l_f while the effect of surface roughness is neglected. It is shown that under a conventional grinding condition (i.e. q = 50-500; a = 0.005- 0.12mm), the real contact length, l_c, can be two to five times the contact length due to the grinding force, l_f. However, if the roughness factor R_r is considered as shown in Figure 4, where $R_r = 9$ is applied, the magnitude of the contact length due to the grinding force and the contact surface roughness (i.e. $l_{rf} = R_r\ l_f$) is approaching that of the real contact length l_c. This demonstrates the effect of the roughness factor R_r on the real contact length, it is, therefore, important to take the R_r factor into consideration when studying the real contact length in grinding. It shows also that if both q and a_e are small, a typical fine/shallow grinding scenario, then the effect of grinding geometry on overall contact length of the wheel/workpiece can be neglected.

The Criterion of Using the Geometric Contact Length l_g. As mentioned before, much previous work ignored the effect of deflection in grinding on the grinding contact length and used the geometry contact length to represent the real contact length. The advantage of this approach is obvious since it makes the analysis simple. For example, Kopalinsky [18] used the geometrical contact length l_g to represent the real contact length l_c in analysing grinding temperatures. In Kopalinsky's work, the contact length was used to quantify several grinding parameters, including the contact area of wheel and workpiece, the size of the heat source and the size of the heat flux of rubbing for calculating the grinding temperatures, the size of a set of active grains on the wheel in contact with the workpiece simultaneously in grinding and the time it took for the set to enter the contact region, the number of active cutting edges in the grinding contact area and the number of active rubbing points in the grinding contact area, and the contact time of individual active cutting grains with the workpiece, which demonstrated the importance of the contact length in the analysis of grinding processes.

Table 2 is a comparison of the results obtained based on the two different treatments on the contact length, using Kopalinsky's data. It shows clearly that by taking the effect of elastic flattening of the wheel, the size of the contact lengths is increased by 86%. And consequently the number of active cutting edges in the grinding contact area becomes 26 instead of 14. By using the overall contact length as the measure of the heat source size for calculating the grinding temperature, the estimated grinding maximum temperature is 26% less than that the elastic flattening of the wheel is neglected, as shown in Table 2.

Table 2 Comparison of the results based on different contact length models

	x based on l_c, Eq.(1)	y based on l_g, Formula (1a)	x/y
Contact length	3.49 mm	1.88 mm	1.855
Contact area	10.5 mm^2	5.64 mm^2	1.855
Number of active edges	26	14	1.855
Maximum grinding temperature [16]	$T_{\max} = \left[\frac{1.2\,\mathrm{Re}_e\, v_w a}{\sqrt{v_w (k\rho c)_w}}\right] \frac{1}{\sqrt{l_c}}$	$T_{\max} = \left[\frac{1.2\,\mathrm{Re}_e\, v_w a}{\sqrt{v_w (k\rho c)_w}}\right] \frac{1}{\sqrt{l_g}}$	0.734

Conditions used in the analysis [18]:
Workpiece martial: En9; Grinding wheel: WA46J with diameter d_s of 177 mm;
Depth of cut a_e: 0.02 mm; Width of cut b: 3 mm:
Wheel speed v_s: 40 m/s; Workpiece speed v_w: 0.5 m/s;
F_n': 10 N/mm; K_s: 6.16 10^{-6} mm^2/N; K_w: 1.36 10^{-6} mm^2/N: $R_r = 9$

Figure 5 is an overview of the contours of $r_{c\text{-}g}$ covering a full range of grinding conditions, from fine grinding, shallow grinding, creep-feed grinding to high speed grinding (i.e. q is from 50 to 10000 and a_e is from 0.001 to 50 mm). The top-right area in the figure, labelled with 'I' (where q and a_e are big), represents those grinding conditions under which the simplification of $l_c = l_g$ is valid, i.e. the simplification only causes an error of 20% or less. The bottom-left area in the figure, labelled with 'III', represents those grinding conditions under which the simplification of $l_c = l_g$ is not valid, i.e. the simplification would cause an error of 200% or more. Under the conditions in the area labelled 'II', the overall contact length l_e can be represented by $l_e = \alpha\, l_g$, where α varies from 1.2 to 3 depending on q and a_e. It is maybe, therefore, sensible to use $l_e = (2\sim3)\, l_g$ as recommended by some researches for simplicity under those grinding conditions.

In summary, normally the effect of elastic flattening of the wheel due to grinding force and the topography of the wheel cannot be neglected and the orthogonal contact length model should be used to quantify the overall grinding contact length. Under large depth of cut and big speed ratio, which is the condition in creep-feed grinding, however, geometrical contact length can be used to represent the real contact length for convenience without lose of accuracy.

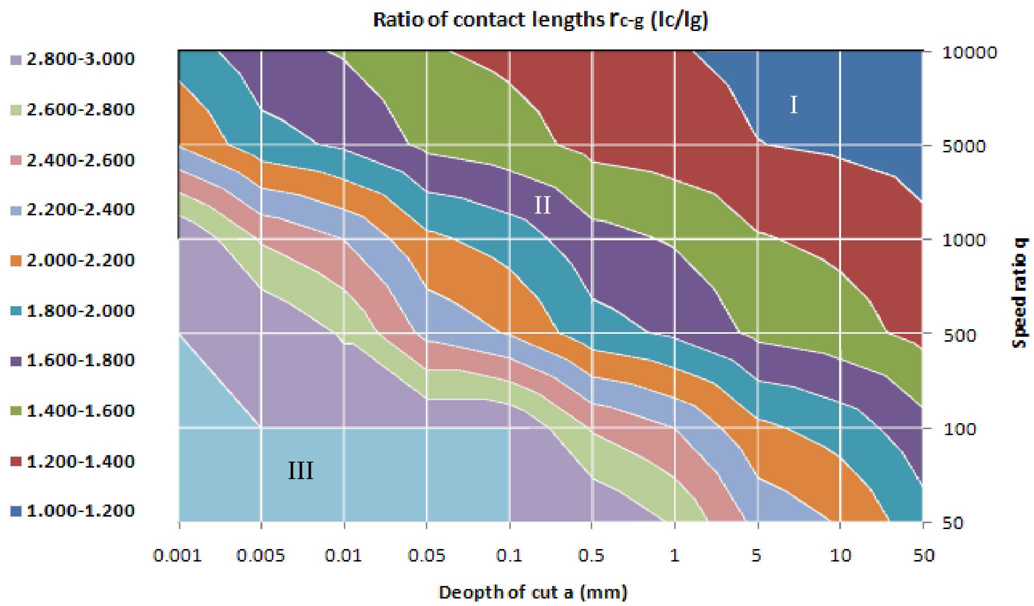

Fig. 5 Contours of the $r_{c\text{-}g}$ vs. depth of cut and speed ratio

Discussion of the Effect of Grinding Wheel Wear.

It is known that grinding force and grinding temperature increase as wheel wear increases [18-20]. Kopalinsky interpreted this phenomenon as due to an increase in negative rake angle of the cutting edges in addition to a growth in area of the wear flats on the grits. As a result the grinding cutting forces could be increased, which was the main reason for the increase of grinding temperatures with wheel wear. In addition, it was known that the increasing rubbing force due to wheel wear and the filling of the voids on the wheel with work material could also contribute to an increase in the workpiece temperature.

Qi's work [20] revealed another possible way by which grinding wheel wear would affect the maximum grinding temperature. It was found, as shown in Figure 6, that increasing the rubbing area due to wheel wear and the filling of the voids on the wheel with work material caused the real depth of cut a_e decrease under the same nominal depth of cut. Figure 6 shows also that the contact of the wheel and workpiece was much concentrated when the grinding wheel became dull. As the result, the overall effective contact length was decreased. The phenomenon can be interpreted by using the orthogonal contact length model Eq.(6). Assuming $e_2 = 0.75$ and taking $K_s = (1 - \nu_s^2)/(\pi\, E_s)$, $K_w = (1 - \nu_w^2)/(\pi\, E_w)$, the Eq.(6) becomes:

$$l_c^2 = l_{rf}^2 + l_g^2$$

and

$$l_{rf}^2 = R_r^2\ 8\ F_0\ a_e^{0.75}\ q^{(-0.5)}\ d_e^{1.25}\ 10^{2.25}\ [(1-\nu_s^2)/(\pi E_s) + (1-\nu_w^2)/(\pi E_w)]$$

$$l_g^2 = a_e\ d_e \qquad (6')$$

Eq.(6') shows clearly that a decrease in a_e or an increase in E_s will cause a decrease in l_c. The mechanisms of grinding wheel wear affecting the effective cutting length can be, therefore, summarised as:

1. The dull edges cause an increase of the cutting rake angle and the rubbing area and decrease the penetration of the active edges into the workpiece under the same normal force, which means the real depth of cut a_e become small, as shown in Figure 6. Consequently, both the geometrical length and the length due to deflection are decreased according Eq.(6') (or l_g, $l_{rf} \propto a_e$).

2. The dull edges and the filling of the voids on the wheel with work material make the grinding wheel stiffer, i.e. the effective stiffness of the wheel (or the hardness of the wheel represented by the wheel modulus E_s) becomes high. According Eq.(6'), the length due to deflection decreases as the increase in the effective wheel modulus E_s (or $l_{rf} \propto 1/E_s$).

According grinding temperature model (as shown in Table 2), the maximum grinding temperature is inverse proportional to the square-root of the heat source size (or $T_{max} \propto 1/l_e$). Therefore, shorter contact length due to wheel wear results in a higher maximum grinding temperature.

In summary, an increase of grinding wheel wear and dullness during grinding processes means not only an increase in the area of the wear flats on its grains, an increase in the negative rake angle of the cutting edges as highlighted by Kopalinsky [18], but also a decrease in the real contact length. All the changes contribute to the grinding temperature increase and the consequent occurrence of thermal damage.

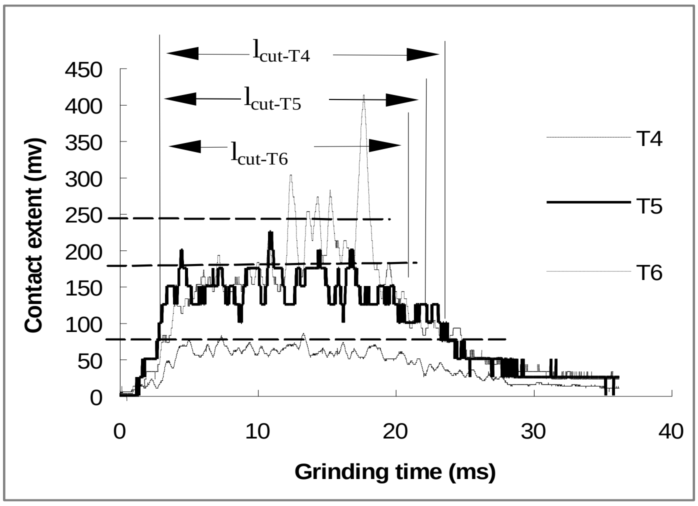

Fig. 6 The change of contact status with different variations of grinding wheel [20].
Test conditions: Cast iron; with coolant; v_w = 0.1 m/s; a = 30 μm;
T4: newly dressed wheel; slight burn a_e = 16 μm;
T5: lightly worn wheel; medium burn a_e = 14 μm;
T6: worn wheel; heavy burn a_e = 12 μm

Conclusions

1. By using specific grinding power, the orthogonal contact length model is modified, which is more suitable for the applications such as on line controls of grinding processes.

2. The orthogonal contact length model is also modified by using a well known empirical force equation, which is capable for predicting the contact length in a wide arrange of grinding conditions. 3. By using the modified orthogonal contact length model, the difference between the overallcontact length and the geometrical contact length as well as the difference between the overall contact length and the contact length due to grinding force are analysed under a wide range of grinding conditions.

4. With a case study, the criterion of using geometric contact length l_g to represent the real contact length l_c, in terms of convenience versus accuracy, is discussed. It is found that in most grinding application condition the magnitude of l_c is up to three times that of l_g depending on the values of q and a_e. Under large depth of cut and high speed ratio, which is the condition of a creep-feed grinding, geometrical contact length can be used to represent the real contact length without lose of accuracy.

5. Grinding wheel wear causes the grinding temperature to increase not only due to its bigger negative rake angle and increased rubbing area, but also due to a shortening of the size of the effective grinding heat source.

References

[1] H.K. Toenshoff, H.G. Wobker, G. Brunner: Annals of the CIRP, Vol. 44 (1995) No.1, pp.311-316.

[2] H.K. Toenshoff, J. Peters, I. Inasaki, T. Paul: Annals of the CIRP, Vol.41 (1992) No.2, pp.677-688.

[3] H.Z. Choi: *Beitrag zur Ursachenanalyse der Randzonenbeeinflussung beim Schleifen*. PhD Dissertation, Universitat Hannover, Germany, 1986.

[4] L. C. Zhang, T. Suto, H. Noguchi and T. Waida: Int. J. Much. Tools Manufact. Vol. 33 (1993) No. 4, pp. 587-597.

[5] Richard P. Lindsay and Robert S. Hahn: The Principles of Grinding, SME Technical Report, (1971), MRR71-01.

[6] R.H. Brown, K. Saito and M.C. Shaw: Annals of the CIRP, Vol.19 (1971), pp.105-113.

[7] K.V. Kumar and M.C. Shaw: Journal of Engineering for Industry, Vol.103 (1981), pp: 73-78.

[8] H. Tsuwa, et al: Journal of Japan Society of Precision Engineering, Vol.41 (1975), pp.358-363.

[9] H. Brandin: *Pendelschleifen und Tiefschleifen Vergleichende Untersuchungen beim Schleifen von Rechteckprofilen*, Dissertation, T.U. Braunschweig, Germany, 1978.

[10] M. Maris: Thermische aspekten van de oppervlakteintegriteit bij het slijpen, Dissertation, Katholieke Universiteit te Leuven, Belgien, 1977.

[11] H.S. Qi, B. Mills and W.B. Rowe: Wear, Vol.176 (1994), pp.137-141.

[12] J.A. Greenwood and J.H. Tripp: Brit. J. Appl. Phys., Vol.17, pp.81-91.

[13] J. Peklenik: Industrie-Anzeiger, Vol.80 (1958), pp.10-17.

[14] W.B. Rowe, H.S. Qi, M.N. Morgan and H.W. Zheng: *The Real Contact Length in Grinding, Based on Depth of Cut and Contact Deflections*, Proc. of the Thirtieth International MATADOR Conference, UMIST, The Macmillan Press Ltd., (1993), pp.187-193.

[15] W.B. Rowe, H.S. Qi, M.N. Morgan and H.W. Zheng: Annals of the CIRP, Vol. 42 (1993) No.1, pp.409-412.

[16] H.S. Qi: *A Contact Length Model for Grinding Wheel - Workpiece Contact*, Ph.D. Thesis, Liverpool John Moores University, UK, 1995.

[17] P.G. Werner: SME Technical Paper, (1979) MR79-319.

[18] E.M. Kopalinsky: Wear, Vol.94 (1984) pp. 295-322.
[19] Malkin, S.: *Grinding Technology*, Ellis Horwood, Chichester, 1998.
[20] H.S. Qi, W.B. Rowe and B. Mills: Key Engineering Materials, Vols. 202-203 (2001), pp:15-24.

Appendix: Notation

a	The nominal depth of cut	mm
a_e	The real depth of cut (the wheel depth of cut)	mm
b	Grinding width	mm
d_e	Equivalent diameter of a grinding wheel	mm
d_s	Diameter of a grinding wheel	mm
d_w	Diameter of a workpiece	mm
E_s	Modulus of elasticity of a grinding wheel	N/mm^2
E_w	Modulus of elasticity of a workpiece	N/mm^2
F_n	Normal grinding force	N
F_n'	The specific normal force, $F_n' = F_n/b$	N/mm
F_t'	The specific tangential force	N/mm
l_c	Theoretical contact length	mm
l_g	Geometric contact length	mm
l_e	Real contact length	mm
l_f	Contact length due to normal force	mm
l_{rf}	$R_r\, l_f$	mm
P’	The specific grinding power, $P' = v_s\, \mu\, F_n'$	Nm/s-mm
q	The speed ratio $q = v_s/v_w$	
R_r	The roughness factor	
r_{c-g}	The contact length ratio between l_c and l_g	
r_{c-rf}	The contact length ratio between l_c and l_{rf}	
v_s	Peripheral wheel speed	m/s
v_w	Table speed or peripheral workpiece speed	m/s
μ	The grinding friction coefficient	
υ_s	Poisson ratio of the grinding wheel	
υ_w	Poisson ratio of the workpiece	